articles

molecular pharmaceutics

Effect of Variations in the Amounts of P-Glycoprotein (ABCB1), BCRP (ABCG2) and CYP3A4 along the Human Small Intestine on PBPK Models for Predicting Intestinal First Pass

Arnaud Bruyère,[†,‡] Xavier Declèves,[†] Francois Bouzom,[‡] Kathryn Ball,[‡] Catie Marques,[†] Xavier Treton,[§] Marc Pocard,[||] Patrice Valleur,[||] Yoram Bouhnik,[§] Yves Panis,[⊥] Jean-Michel Scherrmann,[†] and Stephane Mouly*[,†,#]

INSERM U705-CNRS UMR 7157, Faculté de Pharmacie, Université Paris Descartes, Paris, France, Department of Non-Clinical Modelling, Technologie Servier, Orléans, France, Department of Gastroenterology, Beaujon Hospital, Assistance Publique-Hôpitaux de Paris, Université Paris VII—Denis Diderot, Clichy, France, Department of Digestive Surgery, Lariboisière Hospital, Assistance Publique-Hôpitaux de Paris, Université Paris VII—Denis Diderot, Paris, France, Department of Digestive Surgery, Beaujon Hospital, Assistance Publique-Hôpitaux de Paris, Université Paris VII—Denis Diderot, Clichy, France, and Department of Internal Medicine, Lariboisiere Hospital, Assistance Publique-Hôpitaux de Paris, Université Paris VII—Denis Diderot, Paris, France

Received January 23, 2010; Revised Manuscript Received July 9, 2010; Accepted July 12, 2010

Abstract: It is difficult to predict the first-pass effect in the human intestine due to a lack of scaling factors for correlating *in vitro* and *in vivo* data. We have quantified cytochrome P450/3A4 (CYP3A4) and two ABC transporters, P-glycoprotein (P-gp, ABCB1) and the breast cancer resistant protein BCRP (ABCG2), throughout the human small intestine to determine the scaling factors for predicting clearance from intestinal microsomes and develop a physiologically based pharmacokinetic (PBPK) model. CYP3A4, P-gp and BCRP proteins were quantified by Western blotting and/or enzyme activities in small intestine samples from 19 donors, and mathematical trends of these expressions with intestinal localization were established. Microsome fractions were prepared and used to calculate the amount of microsomal protein per gram of intestine (MPPGI). Our results showed a trend in CYP3A4 expression decrease from the upper to the lower small intestine while P-gp expression is increasing. In contrast, BCRP expression did not vary significantly with position, but varied greatly between individuals. The MPPGI (mg microsomal protein per centimeter intestine) remained constant along the length of the small intestine, at about 1.55 mg/cm. Moreover, intrinsic clearance measured with specific CYP3A4 substrates (midazolam and an in-house Servier drug) and intestinal microsomes was well correlated with the amount of CYP3A4 ($R^2 > 0.91$, $p < 0.01$). *In vivo* data were more accurately predicted using PBPK models of blood concentrations of these two substrates based on the segmental distributions of these enzymes and MPPGI determined in this study. Thus, these mathematical trends can be used to predict drug absorption at different intestinal sites and their metabolism can be predicted with the MPPGI.

Keywords: Cytochrome P450; human intestine; P-gp; BCRP; PBPK; MPPGI

10.1021/mp100015x
Published on Web 07/06/2010

Introduction

Most drugs (over 70%) are administered orally.[1] Hence, the small intestine is a vital barrier to their entry into the systemic circulation. The ability to predict the rate and extent of absorption of orally administered compounds is crucial for improved drug development. Factors such as the small intestine permeability, active uptake and efflux transport, drug metabolism, food effects and solubility all influence the amount of a drug entering the portal vein. Previous *in vitro* and *in vivo* studies have focused on CYP3A-mediated metabolism and P-gp mediated efflux as significant contributors to oral drug bioavailability.

The impact of small intestinal first pass on the overall oral bioavailability of drugs has been carefully studied since 1991[2,3] and is usually included in prediction models. The permeability and metabolism of a drug are key factors for predicting the intestinal first-pass effect, as phase I/phase II drug-metabolizing enzymes and influx/efflux transporters are present all along the human intestinal tract.[4] To date, at least seven CYPs have been identified in the human small intestine by mRNA analysis, protein assays and/or enzyme activity.[5−13] The ATP-binding cassette (ABC) transporters have also been found throughout the human small intestine, but mainly as their mRNAs (especially the *MDR1*, *BCRP* and the *MRP*s mRNAs).[14−19] Mouly et al. (2003)[14] studied four healthy donors and demonstrated that the levels of P-gp increased from the duodenum to the colon. However, there is presently no clear picture of the way in which the abundance of either CYPs or P-gp varies with their location along the human small intestine. Neither is there any clear relationship that can be used to predict intestinal clearance from intrinsic

* Correspondence to this author at Hôpital Lariboisière, Service de Médecine Interne A, 2 rue Ambroise Paré, 75010 Paris, France. Tel: 33-1-49 95 81 27. Fax: 33-1-49 95 84 46. E-mail: stephane.mouly@lrb.aphp.fr.

† Université Paris Descartes.

‡ Technologie Servier.

§ Department of Gastroenterology, Beaujon Hospital, Assistance Publique-Hôpitaux de Paris, Université Paris VII—Denis Diderot.

|| Department of Digestive Surgery, Lariboisière Hospital, Assistance Publique-Hôpitaux de Paris, Université Paris VII—Denis Diderot.

⊥ Department of Digestive Surgery, Beaujon Hospital, Assistance Publique-Hôpitaux de Paris, Université Paris VII—Denis Diderot.

Department of Internal Medicine, Lariboisiere Hospital, Assistance Publique-Hôpitaux de Paris, Université Paris VII—Denis Diderot.

(1) Wilson, C. Gastrointestinal transit and drug absorption. In *Oral drug absorption: Prediction and assessmen*; Dressman, J. B., Lennernäs, H., Ed.; Marcel Dekker: New York, 2000.

(2) Kolars, J.; Awni, W.; Merion, R.; Watkins, P. First-pass metabolism of cyclosporine by the gut. *Lancet* **1991**, *14*, 1488–1490.

(3) Paine, M.; Shen, D.; Kunze, K.; Perkins, J. D.; Marsh, C. L.; McVicar, J. P.; Barr, D. M.; Gillies, B. S.; Thummel, K. E. First-pass metabolism of midazolam by the human intestine. *Clin. Pharmacol. Ther.* **1996**, *60*, 14–24.

(4) Benet, L. Z. The drug transporter-metabolism alliance: uncovering and defining the interplay. *Mol. Pharmaceutics* **2009**, *6*, 1631–1643.

(5) Paine, M.; Khalighi, M.; Fisher, J.; Shen, D. D.; Kunze, K. L.; Marsh, C. L.; Perkins, J. D.; Thummel, K. E. Characterization of interintestinal and intraintestinal variations in human CYP3A-dependent metabolism. *J. Pharmacol. Exp. Ther.* **1997**, *283*, 1552–1562.

(6) Paine, M.; Ludington, S.; Chen, M.; Stewart, P. W.; Huang, S. M.; Watkins, P. B. Do men and women differ in proximal small intestinal CYP3A or P-glycoprotein expression. *Drug Metab. Dispos.* **2005**, *33*, 426–433.

(7) Paine, M.; Hart, H.; Ludington, S.; Haining, R. L.; Rettie, A. E.; Zeldin, D. C. The human intestinal cytochrome P450 "pie". *Drug Metab. Dispos.* **2006**, *34*, 880–886.

(8) Obach, R.; Zhang, Q.; Dunbar, D.; Kaminsky, L. S. Metabolic characterization of the major human small intestinal cytochrome p450s. *Drug Metab. Dispos.* **2001**, *29*, 347–352.

(9) Komura, H.; Iwaki, M. Species differences in *in vitro* and *in vivo* small intestinal metabolism of CYP3A substrates. *J. Pharm. Sci.* **2007**, *97*, 1775–1800.

(10) Madani, S.; Paine, M.; Lewis, L.; Thummel, K. E.; Shen, D. D. Comparison of CYP2D6 content and metoprolol oxidation between microsomes isolated from human livers and small intestines. *Pharm. Res.* **1999**, *16*, 1199–1205.

(11) Lown, K.; Kolars, J.; Thummel, K.; Barnett, J. L.; Kunze, K. L.; Wrighton, S. A.; Watkins, P. B. Interpatient heterogeneity in expression of CYP3A4 and CYP3A5 in small bowel. Lack of prediction by the erythromycin breath test. *Drug Metab. Dispos.* **1994**, *22*, 947–955.

(12) Zhang, Q.; Dunbar, D.; Ostrowska, A.; Zeisloft, S.; Yang, J.; Kaminsky, L. S. Characterization of human small intestinal cytochromes P-450. *Drug Metab. Dispos.* **1999**, *27*, 804–809.

(13) Zeldin, D.; Foley, J.; Goldsworthy, S.; Cook, M. E.; Boyle, J. E.; Ma, J.; Moomaw, C. R.; Tomer, K. B.; Steenbergen, C.; Wu, S. CYP2J subfamily cytochrome P450s in the gastrointestinal tract: expression, localization, and potential functional significance. *Mol. Pharmacol.* **1997**, *51*, 931–943.

(14) Mouly, S.; Paine, M. P-glycoprotein increases from proximal to distal regions of human small intestine. *Pharm. Res.* **2003**, *20*, 1595–1599.

(15) Taipalensuu, J.; Törnblom, H.; Lindberg, G.; Einarsson, C.; Sjöqvist, F.; Melhus, H.; Garberg, P.; Sjöström, B.; Lundgren, B.; Artursson, P. Correlation of gene expression of ten drug efflux proteins of the ATP-binding cassette transporter family in normal human jejunum and in human intestinal epithelial Caco-2 cell monolayers. *J. Pharmacol. Exp. Ther.* **2001**, *299*, 164–170.

(16) Chan, L.; Lowes, S.; Hirst, B. The ABCs of drug transport in intestine and liver: efflux proteins limiting drug absorption and bioavailability. *Eur. J. Pharm. Sci.* **2004**, *21*, 25–51.

(17) Zimmermann, C.; Gutmann, H.; Hruz, P.; Gutzwiller, J. P.; Beglinger, C.; Drewe, J. Mapping of multidrug resistance gene 1 and multidrug resistance-associated protein isoform 1 to 5 mRNA expression along the human intestinal tract. *Drug Metab. Dispos.* **2005**, *33*, 219–224.

(18) Hilgendorf, C.; Ahlin, G.; Seithel, A.; Artursson, P.; Ungell, A. L.; Karlsson, J. Expression of thirty-six drug transporter genes in human intestine, liver, kidney, and organotypic cell lines. *Drug Metab. Dispos.* **2007**, *35*, 1333–1340.

(19) Seithel, A.; Karlsson, J.; Hilgendorf, C.; Björquist, A.; Ungell, A. L. Variability in mRNA expression of ABC- and SLC-transporters in human intestinal cells: comparison between human segments and Caco-2 cells. *Eur. J. Pharm. Sci.* **2006**, *28*, 291–299.

clearance due to a lack of scaling factors for the human small intestine. A scaling factor is known for the liver, and hepatic data have frequently been used to predict intestinal first pass, based on the relative amounts of CYP3A4 in the liver and intestine. But this approach is far from physiological, despite some predictions being similar to observed *in vivo* data.[20] Many software tools are presently available for predicting the first-pass effect and bioavailability of drugs from *in vitro* data. Although prediction models are becoming more and more reliable, particularly the physiologically based pharmacokinetic models (PBPK), they often fail to accurately predict the extent of intestinal metabolism, mainly due to a lack of data on the amount of microsomal protein per gram of intestine (MPPGI) and the concentration of CYP in each of the intestinal segments. PBPK models need to be refined to make them more pertinent. Studies by Paine et al. (2006)[7] and Badhan et al. (2009)[20] have estimated the MPPGI to be 2 mg per gram of gut. This factor is commonly used in the Simcyp PBPK model and considers the intestine to be a homogeneous metabolic organ, with different amount of CYP3A4 along the gastrointestinal tract. However, the intestine is not a homogeneous tissue. Hence, factors such as the segmental distribution of intestinal enzymes and MPPGI need to be accurately determined for each segment of the small intestine.

Although determining these relationships may require several human samples, the resulting data could lead to better prediction of the impact of the intestinal first-pass effect. For example, it could allow the prediction of how orally administered drug are metabolized and thus enable doses to be adjusted to specific pathological conditions. This study focuses on CYP3A4 and P-gp because they are the main proteins involved in the metabolism of over 50% of currently marketed drugs.[22] CYP3A4 also accounts for almost 80% of total intestinal CYPs.[7] In addition, their substrate specificities overlap substantially.[23,24] Thus intestinal CYP3A4 and P-gp may regulate the availability of oral drugs.[24] Lastly, the substrate specificity of BCRP overlaps to a considerable, but varying, degree that of P-gp.[25,26] We therefore determined the distributions of both proteins all along the intestinal tract.

The resulting data were combined to establish a mathematical trend between the amounts of CYP3A4, BCRP and P-gp and the distance from the stomach to the colon. We also measured the enzymatic activities of CYP3A4 in microsomal protein extracts taken along the whole length of the small intestine using midazolam and a Servier company in-house drug. These data were used to determine the MPPGI for each section of intestine, as previously described for the liver.[21]

Finally, we challenged our *in vitro* results and scaling factors with a physiologically based pharmacokinetic (PBPK) model to predict the plasma/blood concentration profiles of oral administered midazolam and the Servier drug. This model uses the newly determined MPPGIs and the segmental expression of CYP3A4 and P-gp.

Patients, Materials and Methods

Chemicals. Midazolam (MDZ), 1′-hydroxy midazolam (1′-OH MDZ), protease inhibitors and organic solvents were purchased from Sigma-Aldrich (St. Louis, MO). The Servier drug (S drug), a specific CYP3A4 substrate, and its hydroxylated primary metabolite were a gift from Technologie Servier (Orleans, France). Midazolam and the Servier company in-house drug (S drug) parameters are detailed in Perdaems et al.[27]

Patients and Tissue Procurement. The collection of human tissues ($n = 9$) and intestinal biopsies ($n = 10$) and their use were approved by the local Ethics Committee of Paris—Hopital Saint Louis. All patients gave written informed consent prior to tissue collection. Duodenal and ileal pinch biopsies were obtained from 10 patients, mean age 58 ± 16 years (range: 33−79 years), undergoing upper and/or lower endoscopy for gastric disorders ($n = 2$), diarrhea ($n = 3$), intestinal transplant ($n = 2$), or polypectomy ($n = 3$) (Table 1). Duodenal, jejunal and ileal samples were collected from 9 patients, mean age 57.5 ± 17 years (range: 36 to 82) during surgery for pancreatic ($n = 3$), intestinal ($n = 2$) or colon cancer ($n = 4$) (Table 1). The "healthy" part of the sample was used; it was taken as far as possible from the tumor, as determined by microscopic examination during surgery. Surgeons evaluated the distance of the sample from the stomach according to the excision protocol. A pool of ileum biopsies was formed from three patients undergoing lower endoscopy for suspected polyps, but all of them were considered healthy, as all donors included in the study. These

(20) Badhan, R.; Penny, J.; Galetin, A.; Houston, B. Methodology for development of a physiological model incorporating CYP3A and P-Glycoprotein for the prediction of intestinal drug absorption. *J. Pharm. Sci.* **2008**, *98*, 2180–2197.

(21) Hakooz, N.; Ito, K.; Rawden, H.; Gill, H.; Lemmers, L.; Boobis, A. R.; Edwards, R. J.; Carlile, D. J.; Lake, B. G.; Houston, J. B. Determination of a human hepatic microsomal scaling factor for predicting in vivo drug clearance. *Pharm. Res.* **2006**, *23*, 533–539.

(22) Zhou, S. Potential strategies for minimizing mechanism-based inhibition of cytochrome P450 3A4. *Curr. Pharm. Des.* **2008**, *14*, 990–1000.

(23) Wacher, V.; Silverman, J.; Zhang, Y.; Benet, L. Z. Role of P-glycoprotein and cytochrome P450 3A in limiting oral absorption of peptides and peptidomimetics. *J. Pharm. Sci.* **1998**, *87*, 1322–1330.

(24) Watkins, P. The barrier function of CYP3A4 and P-glycoprotein in the small bowel. *Adv. Drug Delivery* **1997**, *27*, 161–170.

(25) Doyle, L.; Ross, D. Multidrug resistance mediated by the breast cancer resistance protein BCRP (ABCG2). *Oncogene* **2003**, *22*, 7340–7358.

(26) Haimeur, A.; Conseil, G.; Deeley, R.; Cole, S. P. The MRP-related and BCRP/ABCG2 multidrug resistance proteins: biology, substrate specificity and regulation. *Curr. Drug Metab.* **2004**, *5*, 21–53.

(27) Perdaems, N.; Blasco, H.; Vinson, C.; Chenel, M.; Whalley, S.; Cazade, F.; Bouzom, F. Predictions of Metabolic Drug-Drug Interactions Using Physiologically Based Modelling: Two Cytochrome P450 3A4 Substrates Coadministered with Ketoconazole or Verapamil. *Clin. Pharmacokinet.* **2010**, *49*, 239–258.

Table 1. Intestine Samples[a]

				analysis		
sample	location	type	disease	CYP3A4	P-gp	BCRP
D1	duodenum	biopsy	gastric disorder	WB, microsome	WB	WB
D2	duodenum	biopsy	gastric disorder	WB, microsome	WB	WB
D3	duodenum	surgery	pancreatic cancer	microsome	NA	NA
D4	duodenum	surgery	pancreatic cancer	WB	WB	WB
D5	duodenum	surgery	pancreatic cancer	WB	WB	WB
J1	proximal jejunum	biopsy	gastric disorder	WB	WB	WB
J2	proximal jejunum	surgery	small intestinal cancer	WB, microsome	WB	WB
J3	medium jejunum	surgery	small intestinal cancer	microsome	NA	NA
J4	medium jejunum	biopsy	intestinal transplantation	WB	WB	WB
J5	medium jejunum	biopsy	intestinal transplantation	WB	WB	WB
I1	ileum	biopsy	small intestinal cancer	WB	WB	WB
I2	ileum	surgery	small intestinal cancer	microsome	NA	NA
I3	ileum	surgery	small intestinal cancer	WB, microsome	WB	WB
I4	ileum	surgery	colon cancer	microsome	NA	NA
I5	ileum	surgery	colon cancer	microsome	NA	NA
I6	ileum	biopsy	small intestinal cancer	WB	WB	WB
C1	colon	biopsy	chronic constipation	WB	WB	WB
C2	colon	biopsy	chronic diarrhea	WB	WB	WB
C3	colon	biopsy	polypectomy	WB	WB	WB

[a] NA: Not applicable. WB: Western blot. Microsome: microsomal preparation.

patients were not included in individual analyses. As surgery samples and biopsies were considered as healthy, all samples were comparable. No difference in the protein expression was observed between biopsies and surgery samples, whatever the suspected pathology. Yet, expressions of P-gp, CYP3A4 and BCRP were determined in patients, suggesting that these results have to be interpreted with caution before extrapolating CYP3A4, P-gp and BCRP expression from our patients to patients without intestinal disease.

Preparation of Intestinal Microsomes from Surgical Samples. Intestinal microsomes were prepared using the method developed for rats[28] and adapted for human. Each intestine sample was cooled to 4 °C and immediately washed with 30 mL of 0.9% NaCl, 0.5 mM DTT and a cocktail of protease inhibitors (PI). The sample was placed in a Petri dish and the mucosa scraped off with two microscope slides into phosphate-buffered saline (PBS) solution without calcium and magnesium, 1.5 mM EDTA, 3 UI/mL heparin, 0.5 mM DTT and PI. This tissue was immediately incubated on ice for 20 min in 35 mL of the same solution with horizontal agitation. It was then centrifuged at 900*g* for 10 min, and the resulting pellet was homogenized with a motor-driven Potter-Elvehjem homogenizer in PBS containing 1 mM EDTA, 5 mM histidine, 0.25 mM sucrose and PI (with or without 20% glycerol). This centrifugation/homogenization was repeated. The final pellet was homogenized with the previous buffer (3 mL per gram cells) in a Potter-Elvehjem homogenizer. The resulting homogenate was centrifuged at 10000*g* for 15 min, and the supernatant was ultracentrifuged for 90 min at 100000*g*. The resulting microsomal pellet was homogenized with a Potter-Elvejhem homogenizer in Tris-HCl, pH 7.4 containing PI and stored at −80 °C.

We determined the MPPGI from the weight and length of the tissue sample, the weight of the scraped-off mucosa and total microsomal protein.

The concentrations of microsomal protein were measured using the BC assay (Sigma-Aldrich, St. Louis, MO), and the amount of CYP by the method of Matsubara et al. (1976)[29] and Omura and Sato (1964).[30]

Determination of CYP3A4 Activity in Intestinal Microsomes. Intestinal microsomes (1 mg/mL) in 0.1 mM Tris-HCl, pH 7.4 and 5 mM $MgCl_2$ were incubated at 37 °C with MDZ (0.5 μM) for 30 min; while other microsome samples (2 mg/mL) were incubated with S drug (5 μM) under the same conditions. After a 15 min preincubation, reactions were initiated by adding 1 mM NADPH; they were stopped by adding an equal volume of methanol. Samples were taken at 5 times to obtain linear kinetics. MDZ, S drug and their respective metabolites were separated by high-performance liquid chromatography (HPLC) with an Interchim Symmetry C18 (4.6 × 250 mm) column. The elution gradients were as follows: water/ammonium formate (20 mM) and acetonitrile from 70/30 to 10/90 v/v over 20 min with a plateau from 4 to 10 min at 55/45 v/v. MDZ and S drug were analyzed by liquid chromatography−tandem mass spectrometry (LC−MS/MS); MDZ at transitions 326 > 291.2 *m*/*z* and S drug at 469.3

(28) Bruyere, A.; Decleves, X.; Bouzom, F.; Proust, L.; Martinet, M.; Walther, B.; Parmentier, Y. Development of an optimized procedure for preparation of rat intestinal microsomes: comparison of hepatic and intestinal microsomal cytochrome P450 enzyme activities in two rat strains. *Xenobiotica* **2009**, *39*, 22–32.

(29) Matsubara, T.; Koike, M.; Touchi, A.; Tochino, Y.; Sugeno, K. Quantitative determination of cytochrome P450 in rat liver homogenates. *Anal. Biochem.* **1976**, *75*, 596–603.

(30) Omura, T.; Sato, R. The carbon monoxyde-binding pigment of liver microsomes. *J. Biol. Chem.* **1964**, *239*, 2370–2378.

> 177 *m/z* (positive electrospray ionization). Both activities were quantified from the formation of their respective metabolites normalized to an internal standard. The limit of quantification of MDZ was below 0.001 μM, and that of S drug was below 0.01 μM. Calibration curves were linear over the range studied (5 intermediate concentrations from 0.001 μM to 1 μM for MDZ and from 0.01 to 10 μM for S drug with $R^2 > 0.99$, and CV were less than 5%). An internal standard was used to control injected volume during LC−MS/MS run (injected volume of 100 μL ± 0.5 μL). Intrinsic clearance ($Cl_{int} = V_{max}/K_m$) was calculated from the slope of the plot of substrate disappearance against incubation time (initial conditions). The concentrations used were well below the K_m and were tested to ensure that kinetics were first-order. The slope of substrate disappearance was divided by the protein concentration to obtain an intrinsic clearance in mL/min/g protein.

Western Blotting. The amounts of CYP3A4, P-gp and BCRP proteins along the small intestine were determined in homogenates prepared from intestinal biopsies and surgical samples (from 5 mg of total tissue). The amount of CYP3A4 in the microsomes prepared from each section of the intestine was also measured. Proteins were separated by electrophoresis on 12% sodium dodecyl sulfate polyacrylamide gels (SDS−PAGE) at 100 mV for 1 h (gels for P-gp were 8% SDS−PAGE), and electrotransferred to nitrocellulose membranes at 80 mV for 2 h (samples were analyzed in duplicate on two separate Western blot membranes at two different days). Nonspecific binding sites were blocked by incubation overnight at 4 °C with 5% (w/v) non-fat dried milk in a buffer (TBS-T) containing 10 mM Tris-HCl, pH 7.5, 200 mM NaCl and 0.1% (v/v) Tween 20. The membranes were incubated for 2 h with rabbit or mouse monoclonal antibodies against human CYP3A4 (diluted 1:2000) (Tebu-bio, Le Perray-en-Yvelines, France), P-gp (1:200) (C219 Alexis biochemicals, San Diego, CA), BCRP (1:200) (BXP21 Abcam, Paris, France) and mouse polyclonal antibodies against human CYP3A5 (1:2000) (Tebu-bio, Le Perray-en-Yvelines, France). They were washed with TBS-T and then incubated with enhanced chemiluminescence (ECL) anti-rabbit or anti-mouse secondary horseradish peroxidase-coupled IgG antibody (diluted 1/10000, except for BCRP where antibodies were diluted 1/1000) for one hour (Amersham Biosciences Europe GmbH, Orsay, France) and then washed three times with TBS-T. Membranes were exposed to Amersham ECL blotting detection reagent (ECL; Amersham Biosciences Europe GmbH, Orsay, France) for 5 min. Signals were revealed with the Bio-Rad ChemiDocTM XRS imaging device and the Quantity One 1-D software (BioRad Laboratories, Munich, Germany). The absolute amount of CYP3A4 was determined using supersomes (BD Biosciences, Woburn, MA) as standard (0.025−25 pmol/mg). For P-gp and BCRP, the housekeeping protein β-actin was used to normalize samples and avoid interday variations. A positive control (human liver sample) was added on each Western blot. Western blots were first validated using purified recombinant protein for P-gp and BCRP assays (Abnova, Heidelberg, Germany) and with both supersomes expressed CYP3A4 (BD Gentest, Le Pont de Claix, France) and liver sample for CYP3A4. The reliability of this semiquantitative analysis of protein expression was proven by the linearity of the calibration curve for CYP3A4 (from 0.02 pmol/mg to 20 pmol/mg) and the ratio of the intensities of P-gp or BCRP (from 10 μg to 100 μg per well) divided by that of β-actin. The relationship between the amount of CYP3A4 or the relative abundance of P-gp and BCRP and the position along the human intestine was studied using Sigmaplot software (Systat Software, San Jose, CA). The abundance of P-gp and BCRP was expressed as a relative value with the reference being a pool of ileal tissue from three patients. Therefore, before comparison with the pool, each individual data was normalized with the housekeeping protein β-actin. The pylorus was considered to be the start of the intestine (0 cm), and the jejunum was assumed to start 25 cm after the pylorus. The best mathematical function (linear, exponential, logarithmic and inverse) was selected on the basis of the R^2.

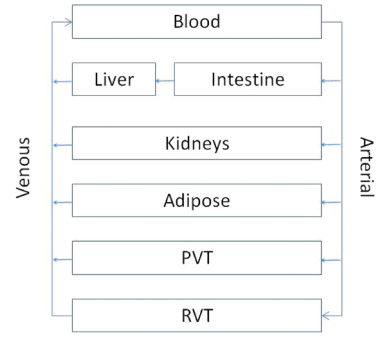

Figure 1. Representation of the PBPK model build to predict *in vivo* data of midazolam and S drug.

PBPK Modeling. The model was built with ASCLXtrem software (The AEgis Technologies Group Inc., Huntsville, AL). The parameters of each molecule and the equations used in the model have been described by Perdaems et al.[27] Both drugs were studied in solution, and as a consequence no dissolution equation was included in the model. Briefly, the absorption, distribution, the liver and intestinal first-pass metabolism and elimination of a drug are predicted by the software (Figure 1). The model differs from that of Perdams et al.[27] in that the gastrointestinal tract was divided into seven sections (1 for the stomach, 1 for the duodenum, 2 for the jejunum, 2 for the ileum and 1 for the colon). Simulations were performed using a model man (70 kg body weight; cardiac blood flow 363 L/h). Organ volumes were expressed as a percentage of body weight and organ blood flows as a percentage of the cardiac blood flow.[27–31 32] The assumptions for the model were as follows: (a) intercompartmental transport occurred via the blood, (b) drug concentrations in

(31) Davies, B.; Morris, T. Physiological parameters in laboratory animals and humans. *Pharm. Res.* **1993**, *10*, 1093–1095.
(32) Brown, R. P.; Delp, M. D.; Lindstedt, S. L.; Rhomberg, L. R.; Beliles, R. P. Physiological parameter values for physiologically based pharmacokinetic models. *Toxicol. Ind. Health* **1997**, *13*, 407–484.

effluent blood and blood within tissues were equal, (c) there was instantaneous equilibrium between tissue and blood within the tissue, and (d) only unbound drugs were eliminated. The model was based on a well-stirred model for all organs and intestinal sections.

The metabolism was evaluated from microsomes according to the following equations:

$$\mathrm{Cl_{liver}} = \frac{\mathrm{Cl_{int(liver)}} \times \mathrm{MPPGL} \times \mathrm{weight_{liver}} \times Q_{\mathrm{liver}} \times f_{\mathrm{u}}}{Q_{\mathrm{liver}} + f_{\mathrm{u}} \times \mathrm{Cl_{int(liver)}} \times \mathrm{MPPGL} \times \mathrm{weight_{liver}}} \quad (1)$$

and

$$\mathrm{Cl_{duodenum}} = \frac{\mathrm{Cl_{int(duodenum)}} \times \mathrm{MPPGI_{duodenum}} \times \mathrm{weight_{duodenum}} \times Q_{\mathrm{duodenum}} \times f_{\mathrm{u}}}{Q_{\mathrm{duodenum}} + f_{\mathrm{u}} \times \mathrm{Cl_{int(duodenum)}} \times \mathrm{MPPGI_{duodenum}} \times \mathrm{weight_{duodenum}}} \quad (2)$$

and

$$\mathrm{Cl_{intestine}} = \mathrm{Cl_{duodenum}} + \mathrm{Cl_{jejunum}} + \mathrm{Cl_{ileum}} + \mathrm{Cl_{colon}} \quad (3)$$

where MPPGL is microsomal protein per gram of liver, MPPGI is the amount of microsomal protein per gram of intestine, $\mathrm{weight_{liver}}$ and $\mathrm{weight_{intestine}}$ are the weights of these organs, Q is the blood flow within the tissue, f_{u} is the unbound fraction (1 in the intestine), $\mathrm{Cl_{int(liver)}}$ is the intrinsic clearance measured on liver microsomes and $\mathrm{Cl_{int(duodenum)}}$ is the intrinsic clearance measured on duodenum microsomes.

Results

Quantification of CYP3A4, P-gp and BCRP in Human Intestinal Samples. The amounts of CYP3A4 in biopsies and surgical samples were determined using 5 mg of intestinal tissue. The mean amount of CYP3A4 in 4 samples of duodenum was 1.74 ± 0.83 pmol/mg total protein (Table 2), showing the great interindividual variations in the concentration of CYP3A4 (CV = 47%). The concentration of CYP3A4 in the jejunum was 3-fold lower than that in the duodenum; the mean concentration was 0.53 ± 0.42 pmol/mg (CV = 77%) total protein. The concentration of CYP3A4 in the proximal jejunum was close to that in the duodenum and roughly 3 times higher than in the medium jejunum; it was below the limit of quantification (<0.02 pmol) in both the ileum and the colon (Table 2). Analysis of all the individual data indicated that the segmental expression of CYP3A4 protein along the small and large intestine is best described by the following logarithmic eq i ($R^2 = 0.89$, Figure 2A):

$$\text{abundance(CYP3A4)} = 0.462 - 0.3353 \times \mathrm{Ln}(\text{distance from pylorus}) \quad \text{(i)}$$

CYP3A5 protein was detected in the duodenal sample from only one Caucasian.

Table 2. Amounts of CYP3A4, P-gp and BCRP in Intestinal Biopsies and Surgical Samples (after Doing Pinch Biopsies)[a]

sample	CYP3A4 (pmol/mg)	P-gp (rel to ileum)	BCRP (rel to ileum)
D1	1.60	0.24	0.72
D2	2.11	0.19	0.37
D4	2.61	0.05	0.98
D5	0.64	ND	ND
J1	1.07	0.53	0.35
J2	0.63	0.60	0.55
J4	0.12	0.87	0.19
J5	0.32	0.77	1.22
I1	BLQ	0.94	1.00
I3	BLQ	1.33	0.43
I6	BLQ	0.79	0.43
C1	BLQ	1.80	0.14
C2	BLQ	1.54	0.61
C3	BLQ	2.13	0.38

[a] Total proteins used in Western blotting experiments were prepared from 5 mg of total tissues. For P-gp and BCRP, results are the relative amounts of P-gp and BCRP in all samples as compared to a pool of ileum, which was set at unity. BLQ stands for below the limit of CYP3A4 quantification (0.02 pmol/mg) ND: not determined.

The abundance of P-gp was expressed relative to the reference pool of ileal tissue from three patients. P-gp was found in all intestinal segments and, unlike CYP3A4, its expression increased about 10-fold from the duodenum (mean = 0.161 ± 0.038, $n = 3$) to the colon (mean = 1.82 ± 0.30, $n = 3$). The expression of P-gp was lowest in the duodenum (50% of the amount in the ileum) and highest in the distal ileum (Table 2). The interindividual variation of P-gp was 3-fold in the duodenum ($n = 3$), 1.4-fold in the jejunum ($n = 4$), and 2-fold in the ileum ($n = 3$) (Figure 2B). Analysis of the individual data indicated that the intestinal segmental distribution of P-gp is best described by the following logarithmic eq ii ($R^2 = 0.76$, Figure 2B):

$$\text{relative abundance (P-gp)} = 0.8772 + 0.3334 \times \mathrm{Ln}(\text{distance from pylorus}) \quad \text{(ii)}$$

The expression of BCRP protein in a particular segment of the intestine varied greatly between individuals (Table 2); it varied 2.4-fold in the duodenum ($n = 3$) and proximal jejunum ($n = 2$), 6-fold at the end of the jejunum ($n = 2$), 3-fold in the ileum ($n = 3$) and 6-fold in the colon ($n = 3$). There was no gradient along the length of the small intestine and the expression of BCRP in the colon was about half that of the small intestine (Table 2).

Determination of MPPGI from Microsomes Prepared from Surgical Samples. MPPGIs are basic data by which intrinsic clearance calculated from intestinal microsomes can be extrapolated to total intestinal clearance using eq 2. The scaling factors for each segment of small intestine are shown in Table 3. The weights of mucosa removed from the samples of intestine were very similar along the whole length of the small intestine. However, the weight of the samples them-

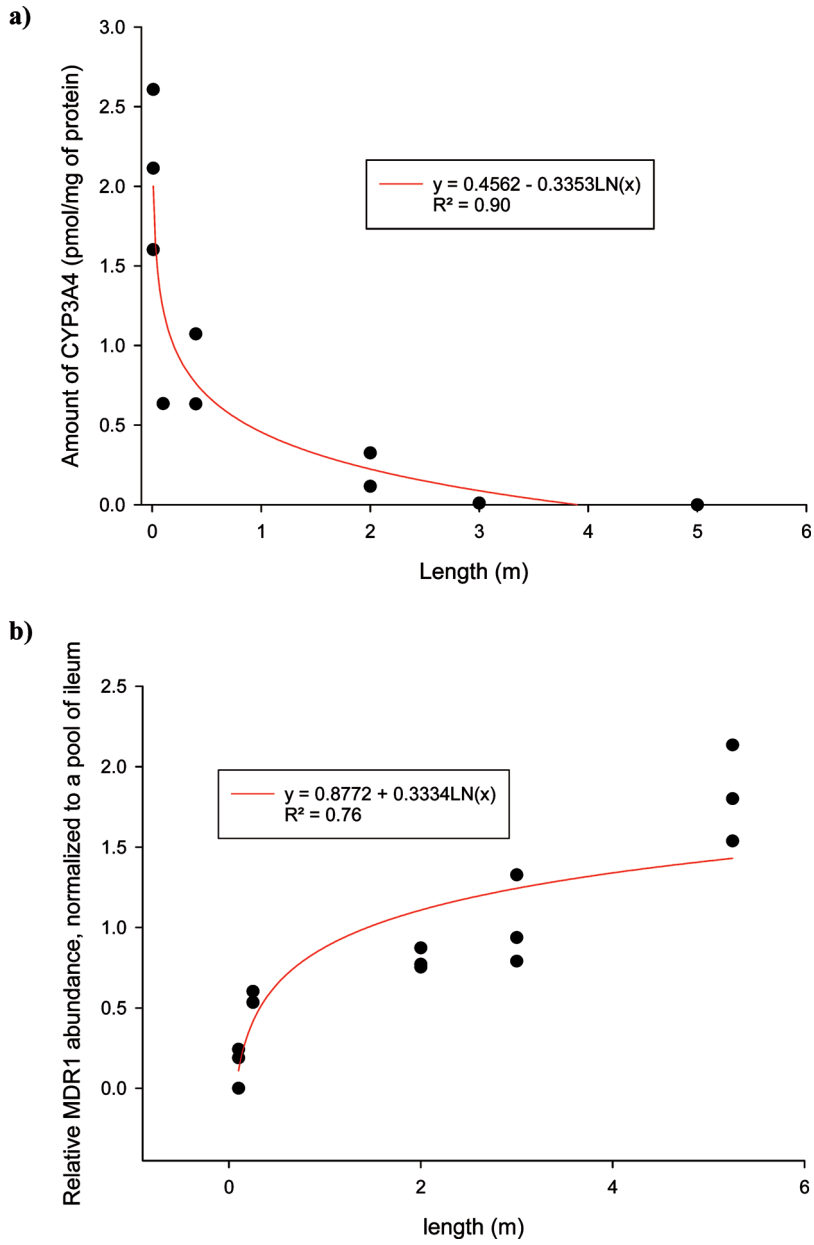

Figure 2. Amounts of CYP3A4 (a) and P-gp (b) along the human intestinal epithelium (from 13 biopsies or scraped tissues). CYP3A4 data that were below the limit of quantification (BLQ) were included as BLQ/2 (0.01 pmol/mg of protein).

Table 3. Determination of MPPGI Factors from Human Intestinal Microsomes (Surgical Samples)[a]

location	mg of microsomal proteins/g of mucosa	g of mucosa/g of intestine	mg of microsomal protein/g of intestine	wt of tissue (g)/cm of intestine	mg of microsomal protein/cm
duodenum (D1, D2, D3)	1.54 ± 0.55	0.24 ± 0.02	0.37 ± 0.12	4.45 ± 0.57	1.59 ± 0.35
jejunum (J2, J3)	2.00 ± 0.08	0.20 ± 0.03	0.37 ± 0.07	4.19 ± 0.68	1.54 ± 0.03
ileum (I2, I3, I4, I5)	2.48 ± 0.71	0.21 ± 0.04	0.54 ± 0.24	3.10 ± 1.09	1.53 ± 0.45

[a] Data presented are means ± SD.

selves decreased from the duodenum to the ileum. Thus, the MPPGI seemed to be constant in terms of the weight of microsomal protein per centimeter of intestine, but it increased 1.6-fold when expressed as microsomal protein per gram of mucosa. The MPPGI was 1.54 to 2.48 mg/g mucosa; far smaller than that of human liver microsomes.

CYP3A4 Level and Metabolic Activity in Intestinal Microsomes. The mean of the amount of CYP3A4 in intestinal microsomes from 3 duodena (D3, D4, D5) was 0.034 nmol/mg, 6 times greater than in the jejunum (0.0058 nmol/mg from J2 and J3) (Table 4). CYP3A4 was detected in only one ileum sample (I2), where it was lower than in

Table 4. CYP3A4 in Human Small Intestinal Microsomes (Surgical Samples)

sample	protein (mg/mL)	CYP450 (nmol/mg)[a]	CYP3A4 (nmol/mg)[c]
D3	18.80	0.106	0.0634
D4	8.60	BLQ[c]	0.0176
D5	3.10	0.147	0.0208
J2	5.46	0.031	0.0074
J3	3.40	BLQ	0.0042
I2	4.60	BLQ	0.0026
I3	5.78	BLQ	BLQ
I4	4.47	BLQ	BLQ
I5	6.09	BLQ	BLQ

[a] Total CYP450 determined spectrophotometrically. [b] CYP3A4 determined by quantitative Western blotting. [c] BLQ: below the limit of quantification (<0.02 nmol/mg for total CYP and <0. 025 pmol/mg for CYP3A4).

Table 5. Intestinal Microsomal Intrinsic Clearance (mL/min/g protein) of Two CYP3A4 Substrates (MDZ and S Drug)[a]

sample	D3	D4	D5	J2	J3	I2	I3	I4	I5
MDZ	21.4	6.7	9.2	4.2	4.5	ND	0.03	ND	ND
S drug	4.9	1.7	2.9	1.1	0.3	ND	ND	ND	ND

[a] Data are means of at least three experiments. Coefficient of variation remained below 5% in all experiments. ND: not detected. Limit of quantification of intestinal clearance was 0.0075 mL/min/g for MDZ and 0.01 mL/min/g for S drug.

the jejunum. We measured the intrinsic clearances of MDZ and S drug in human intestinal microsomes in order to correlate the amount of CYP3A4 with its metabolic activity (Table 5). Cl_{int} were closely correlated ($R^2 > 0.91$ for the appropriate drug) with the CYP3A4 content (Figure 3). Intestinal clearance was calculated from Table 3 and Table 5.

For example, the duodenal clearance of MDZ for a 70 kg healthy man calculated from the present results was

$$Cl_{duo(mdz)} = \frac{21.4 \times 1000 \times 0.37 \times 0.026/100 \times 70 \times 1.6/100 \times 363 \times 1}{1.6/100 \times 363 + 1 \times 21.4 \times 1000 \times 0.37 \times 0.026/100 \times 70}$$

$$Cl_{duo(mdz)} = 5.58 \text{ L/h}$$

Using the same equation and assumptions, $Cl_{jejunum(mdz)}$ was 17.15 L/h and $Cl_{ileum(mdz)}$ was 0.59 L/h, giving a total intestinal clearance of 23.32 L/h. $Cl_{liver(mdz)}$ was also evaluated from the data published by Walsky and Obach (2004)[33] at

$$Cl_{liver(mdz)} = \frac{0.537 \times 1000 \times 40 \times 2.43/100 \times 70 \times 24.79/100 \times 363 \times 0.016}{24.79/100 \times 363 + 0.016 \times 0.537 \times 1000 \times 40 \times 2.43/100 \times 70}$$

$$Cl_{liver(mdz)} = 77.98 \text{ L/h}$$

Hence, the total intestinal clearance of midazolam was about 3 times lower than total liver clearance of midazolam 1′-hydroxylation.

Refinement of PBPK Modeling with MPPGIs and Intestinal CYP3A4 and P-gp Expressions. The blood concentrations of midazolam were used with the PBPK model built with ACSLXtrem, the data from Paine et al.[5] and the relative CYP3A4 amounts in the intestine and liver to determine intestinal metabolism of the drug. The predicted results were closed to the *in vivo* data (Table 6). The intestine extracted about 40% of a 6 mg per os dose, close to the *in vivo* intestinal extraction determined by Paine et al.[3] However, the predicted fraction of an oral dose of 10 mg S drug extracted under the same conditions was only 7%, whereas the *in vivo* data gave a value of 20% (data from Technologie Servier). Therefore, the PBPK model was improved by using the data for CYP3A4 and P-gp obtained in this study and the original MPPGI instead of the relationship between the amounts of CYP3A4 in the liver and intestine.

The predictions of the blood concentrations of both substrates in a 70 kg man are close to the *in vivo* data obtained using the mean Cl_{int} measured with intestinal microsomes (Figure 4 and Table 6). The intestinal metabolism of midazolam was about 40% (2.6 mg for an initial dose of 6 mg) while hepatic metabolism accounted for 55% (3.3 mg for an initial dose of 6 mg) of total metabolism (Figure 5A). The predicted C_{max} of midazolam was 19 μg/mL, while the observed C_{max} was 14 $\pm$ 7 μg/mL; the predicted AUC was 40 μg h/L, while the observed AUC was 75 $\pm$ 47 μg h/L.

Intestinal metabolism accounted for 15% (1.5 mg for an initial dose of 10 mg), while hepatic metabolism accounted for about 75% (7.45 mg for an initial dose of 10 mg) of the total elimination of S drug (Figure 5B). The other route of elimination was renal. The predicted C_{max} of S drug was 68 μg/mL, while the observed C_{max} was 53 $\pm$ 18 μg/mL; the predicted AUC was 144 μg h/L, while the observed AUC was 149 $\pm$ 56 μg h/L.

Discussion

It is presently difficult to predict the plasma pharmacokinetics of an orally administered drug. Many factors must be taken into account: physiological parameters, solubility, permeability, metabolism and transport (efflux/influx), plus the effect of food. Intestinal absorption of a drug not only is modulated by passive diffusion ("permeability") but also represents the net transport of uptake, efflux (P-gp for instance) and/or diffusion or paracellular transport and metabolism, especially by CYP3A4.[23,34] Any prediction of oral bioavailability should include the intestinal distribution of transporters and enzymes in order to accurately take into account the physiology of the GI tract. The intestinal clearance, which reflects both permeability and metabolism, depends on the intrinsic intestinal clearance. This in turn requires the determination of scaling factors with which to

(33) Walsky, R. L.; Obach, R. S. Validated assays for human cytochrome P450 activities. *Drug Metab. Dispos.* **2004**, *32*, 647–660.

(34) Benet, L.; Izumi, T.; Zhang, Y.; Silverman, J.; Wacher, V. Intestinal MDR transport proteins and P450 enzymes as barriers to oral drug delivery. *J. Controlled Release* **1999**, *62*, 25–31.

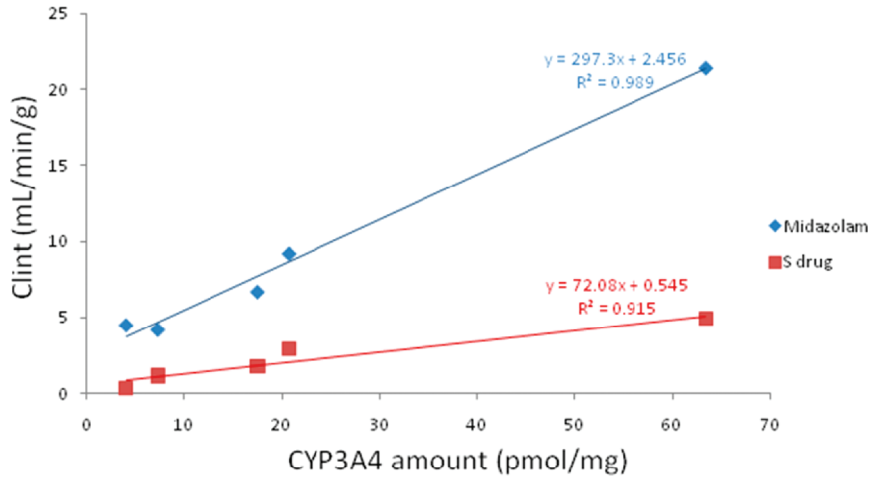

Figure 3. Correlation between midazolam and S drug Cl_{int} and the amount of CYP3A4 as determined in small intestinal microsomes obtained from various parts of the human small intestine after surgery (Table 1).

Table 6. Human Pharmacokinetics of MDZ and S Drug Observed and Predicted Using PBPK Models

	MDZ			S drug		
	predicted			predicted		
parameter	with previous data[a]	with data from this study[b]	obsd *in vivo* PK	with previous data[a]	with data from this study	obsd *in vivo* PK
C_{max} (μg/mL)	15	19	14 ± 7	73	68	53 ± 18
AUC (μg.h/L)	65	40	75 ± 47	202	144	149 ± 56
$t_{1/2}$ (h)	5.0	4.9	5.4 ± 3.0	2.12	1.5	2.9 ± 1.1
intestinal extraction (%)	40	40	40 to 60[3]	7	15	20 ± 9

[a] Prediction using data from Paine et al. (1997)[5] and relative amounts of CYP3A4 in the intestinal segment and liver. [b] Prediction using current data for the amounts of CYP3A4 and P-gp, activities from intestinal microsomes and original MPPGI.

transpose intrinsic clearance determined with intestinal microsomes to total intestinal clearance.

The concentrations of CYP and the main ABC drug transporters along the small intestine have been mapped over the past few years,[5–7,14,35] and all data indicate that the distribution is not uniform in the various intestinal segments. The amount of CYP3A4 decreases from the duodenum to the ileum,[7] and the level of P-gp increases from the duodenum to the ileum.[14] However, there was no clear picture of the mathematical relationships between the quantities of these proteins and the position along the human small intestine. Similarly it was difficult to accurately predict intestinal clearance as the "microsomal protein per gram of intestine" (MPPGI) had not been clearly measured. The studies of Paine et al. (2006)[7] and Badhan et al. (2009)[20] indicated that the MPPGI was about 2 mg/g of gut, but it had never been measured directly.

We have now determined the absolute amounts and activities of CYP3A4 and the relative amounts of P-gp and BCRP in pinch biopsies and scraped-off mucosa (and microsomes for CYP3A4) taken from all along the human small intestine. All samples were considered to be healthy by the surgeon although they came from patients suffering from cancer, gastric disorders or polypectomy. Indeed, previous study has shown no difference in the amounts of CYP3A4 and P-gp in normal and cancer tissues.[36] Besides, two other studies also demonstrated that intestinal P-gp expression in cancer tissue did not change from normal tissues.[37,38] As a consequence, the current data could be considered as the reflection of normal tissue. The segmental distributions of CYP3A4, P-gp and BCRP were accurately mapped so as to give a precise trend between their amounts and the segments of the human small intestine. The microsome preparations were used to calculate scaling factors for each section of the intestine, which could then be used to extrapolate intestinal intrinsic clearance to total intestine

(35) Englund, G.; Rorsman, F.; Rönnblom, A.; Karlbom, U.; Lazorova, L.; Gråsjö, J.; Kindmark, A.; Artursson, P. Regional levels of drug transporters along the human intestinal tract: co-expression of ABC and SLC transporters and comparison with Caco-2 cells. *Eur. J. Pharm. Sci.* **2006**, *29*, 269–277.

(36) Canaparo, R.; Nordmark, A.; Finnström, N.; Lundgren, S.; Seidegård, J.; Jeppsson, B.; Edwards, R. J.; Boobis, A. R.; Rane, A. Expression of cytochromes P450 3A and P-glycoprotein in human large intestine in paired tumour and normal samples. *Basic Clin. Pharmacol. Toxicol.* **2007**, *100*, 240–248.

(37) Hinoshita, E.; Uchiumi, T.; Taguchi, K.; Kinukawa, N.; Tsuneyoshi, M.; Maehara, Y.; Sugimachi, K.; Kuwano, M. Increased Expression of an ATP-binding Cassette Superfamily Transporter, Multidrug Resistance Protein 2, in Human Colorectal Carcinomas. *Clin. Cancer Res.* **2000**, *6*, 2401–2407.

(38) Mizoguchi, T.; Yamada, K.; Furukawa, T.; Hidaka, K.; Hisatsugu, T.; Shimazu, H.; Tsuruo, T.; Sumizawa, T.; Akiyama, S. Expression of the MDR1 gene in human gastric and colorectal carcinomas. *J. Natl. Cancer Inst.* **1990**, *82*, 1679–1683.

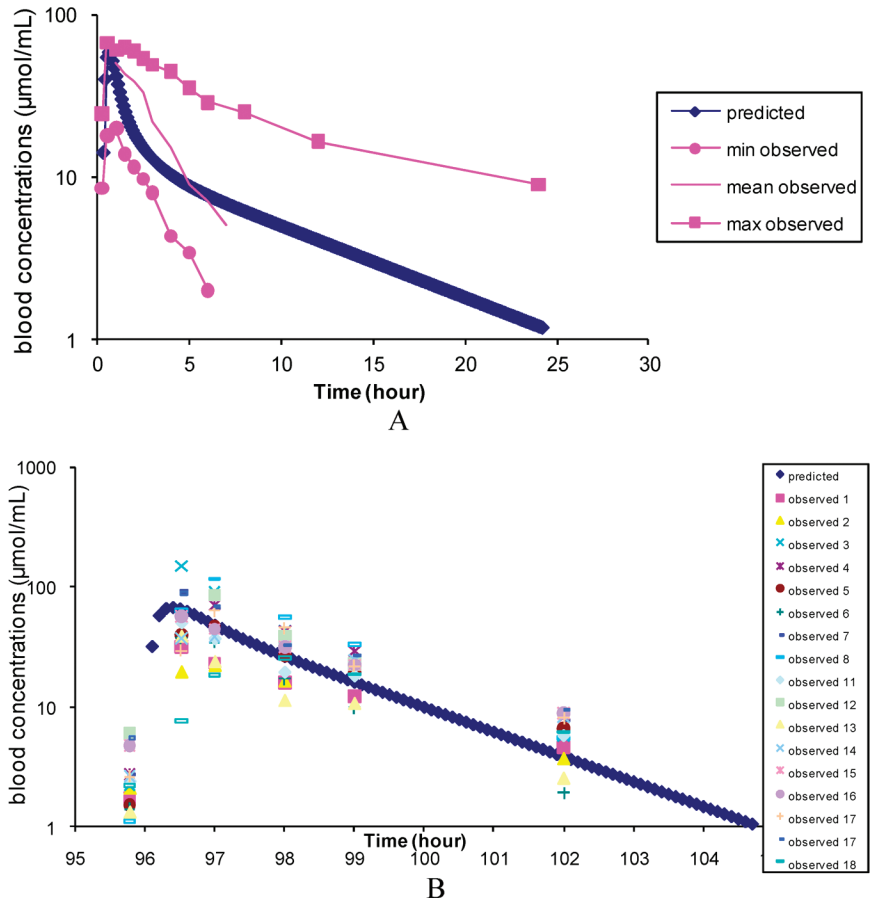

Figure 4. Observed and predicted blood concentrations of midazolam (A) and S drug (B) after an oral dose of 6 mg and 10 mg, respectively, administered to a 70 kg body weight healthy man. Observed data for midazolam are represented by the maximal observed blood concentrations, the mean observed blood concentrations and the minimal observed blood concentrations from *in vivo* data. S drug observed data came from 18 *in vivo* data (observed 1 to 18). All data were obtained from Technologie Servier.

clearance. *Ex vivo* quantification and MPPGIs were used to refine a PBPK model to predict the intestinal metabolism of midazolam and S drug.

The expression of P-gp increased logarithmically from the duodenum to the colon, while that of CYP3A4 decreased. The intrinsic clearances of midazolam and S drug were directly linked to the amount of CYP3A4 protein, which further emphasizes that the amount of CYP3A4 protein accurately reflects enzyme activity (Figure 3). It may now be possible to use microsomes prepared from any segment of the human intestine and the logarithmic trends described here to get an accurate idea of the impact of CYP3A4 on drug absorption, wherever the drug is absorbed. For instance, microsomes from the upper jejunum could be used to determine the ratio between CYP3A4 activity measured using a reference compound and the amount of CYP3A4 protein. The intrinsic clearance or V_{max} of the test compound could then be extrapolated from the profile of CYP3A4 protein and its activity to the rest of the small intestine. Of course, microsomes from the terminal ileum have no activity and could not be transposed to the rest of the small intestine. Such an approach allows predicting intestinal metabolism and absorption of both CYP3A4 and P-gp substrates.

The newly determined scaling factors should lead to more accurate and physiological predictions of total intestinal clearance from intrinsic clearance measured on intestinal microsomes. It will thus be simpler to predict intestinal clearance. The Cl_{int} determined with intestinal microsomes from any part of the duodenum or jejunum could be extrapolated to the intrinsic clearance and then to the whole length of the intestinal tract with the mathematical trend described here. Finally, it should be easy to extrapolate the whole intrinsic clearance to total intestinal clearance with a scaling factor (MPPGI) for each segment.

Intestinal clearance was usually predicted using a MPPGI of 2 mg of microsomal protein per gram of total gut. But a single MPPGI cannot be used for all the intestinal segments as it is not constant along the human small intestine. The intestine cannot not be considered to be a single metabolic organ; there are at least three metabolic sections, each with its own MPPGI. Our data indicate that the value of 2 mg of microsomal protein per gram of intestine is relevant only for the jejunum. This factor is 1.55 for drugs absorbed in the duodenum, and almost 2.5 for the ileum. And there is very little interindividual variation of the MPPGI. These

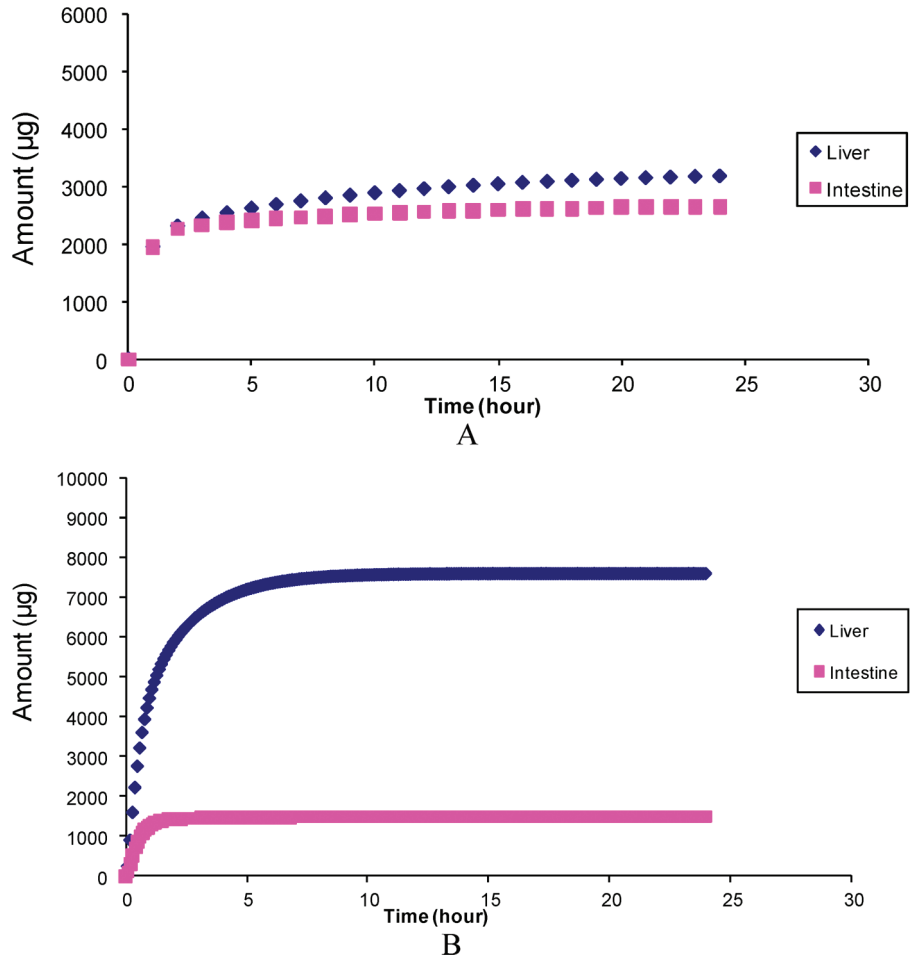

Figure 5. Predicted intestinal (blue curve) and hepatic (red curve) amount of metabolized midazolam (A) and S drug (B) after an oral dose of 6 mg and 10 mg, respectively. Predictions were established for a standard 70 kg man and were the consequences of blood predicted concentrations from Figure 4.

scaling factors are relevant for enzymes located in membranes such as cytochromes but not transporters or soluble enzymes.

These new scaling factors and mathematical trends appear to be relevant, as the current PBPK models including the intestinal first-pass effect agree well with *in vivo* data and predict the impact of both intestinal metabolism and efflux. The intestinal impact on midazolam absorption was well predicted without including these results in the model, but not that of the S drug. This confirms that oral bioavailability cannot be well predicted from hepatic data alone (a simple relationship between the amount of CYP3A4 in the intestine and liver) but needs to include studies supporting drug transport and using optimized PBPK models taking into account intestinal transport. Indeed, there are several *in vitro* methods used to identify P-gp substrates but they are not able to predict the extent to which the *in vitro* data can predict the impact of P-gp in *in vivo* drug absorption.

One of our main findings is that the total intrinsic intestinal clearance of midazolam calculated from eqs 2 and 3 is about three times smaller than the intrinsic hepatic clearance. However, both the *in vivo* data and the PBPK model show that the extraction of midazolam in the intestine and hepatic metabolism are similar. This discrepancy between the intestinal intrinsic clearance calculated from eqs 2 and 3 and the total intestinal metabolism determined with the PBPK model shows that the classical determination of clearance from intrinsic clearance is not enough to predict the impact of intestine in the overall bioavailability *in vivo*. Permeability is not sufficiently taken into account in the calculation. Thus, the impact of intestinal metabolism is better predicted using PBPK models than by using only a calculated intrinsic clearance in order to integrate the influence of permeability into intestinal clearance. This point emphasizes the importance of a physiological approach.

Unfortunately, the impact of BCRP on overall absorption remains difficult to predict. The expression of BCRP, another efflux transporter involved in the transport of compounds such as methotrexate,[39] epirubicine[25] and topotecan, does not vary along the length of the small intestine, but it does vary greatly from one individual to another. As a consequence, the influence of BCRP on the metabolism of a drug

(39) Chen, Z.; Robey, R.; Belinski, M.; Shchaveleva, I.; Ren, X. Q.; Sugimoto, Y.; Ross, D. D.; Bates, S. E.; Kruh, G. D. Transport of methotrexate polyglutamates and 17βestradiol 17-(β-D-glucuronide) by ABCG2: effects of acquired mutations at R482 on methotrexate transport. *Cancer Res.* **2003**, *63*, 4048–4054.

should be constant all the whole length of the small intestine for one person, but predicting its effect for a population will be difficult due to the great interindividual variation. The expression of BCRP varied 6-fold between patients. This large interindividual variation may explain why it is difficult to find the right dose of drugs that are BCRP substrates. For example, low doses of the BCRP substrate methotrexate are commonly used to treat autoimmune and lymphoproliferative diseases.[39] Interindividual variations in BCRP level may explain the observed variability of oral low-dose methotrexate pharmacokinetics,[40−42] although uptake transporters that were not assessed in the current study may also play a role.[43] The many single nucleotide polymorphisms of ABCG2, which alter its activity, may be another source of variation in pharmacological responses.[44]

The mathematical trends and interindividual variations could also be used to better determine the impact of intestinal first pass on total drug bioavailability. Such an *in silico* approach may help determine the influence of the interindividual variations in the amounts of CYP3A4 described here (and previously by Paine et al.)[6] and P-gp (consistent with data from Mouly et al.)[14] on the systemic exposure to oral drugs. We believe that this study on the pharmacokinetics of midazolam and S drug has shown that a combination of new original mathematical trends for determining the concentrations of the enzymes and transporters involved in the distribution of orally administered drugs, new MPPGIs, physiological data (absorption areas, transit times, intestinal pH, etc), and drug chemical properties (pK_a, solubility, dissolution rates, etc.) will improve the prediction of oral drug delivery in both preclinical and clinical settings (using prediction software like ACSLXtrem). Changes in protein concentration along the small intestine may also influence systemic or intestinal diseases, as does Simcyp, but with greater accuracy.

This approach could also be extended to studies on other intestinal enzymes, such as the uridine diphosphate-glucuronosyltransferases[45] and transporters like the multidrug resistance-associated proteins (MRPs),[16,19,35,46] or the various members of the solute carrier superfamily.[35,47] These enzymes and transporters are now known to influence the intestinal barrier and should be introduced in further studies to obtain better physiological models.

In conclusion, we have measured the amounts of CYP3A4, P-gp, and BCRP all along the human small intestine, determined scaling factors needed to predict intestinal clearance from intrinsic clearance, and built an improved PBPK model that includes all these data. The simple mathematical trends described here can also be used to predict drug absorption at different sites along the intestine.

Abbreviations Used

1′-OH MDZ, 1′-hydroxymidazolam; ABC, ATP-binding cassette; AUC, area under the curve; BCRP, breast cancer resistant protein; BLQ, below the limit of quantification; Cl_{int}, intrinsic clearance; CYP, cytochrome P450; ECL, enhanced chemiluminescence; IVIVE, *in vitro*/*in vivo* extrapolation; LC−MS/MS, liquid chromatography−tandem mass spectrometry; MDZ, midazolam; MPPGI, microsomal protein per gram of intestine; ND, not detected; PBPK, physiologically based pharmacokinetics; P-gp, P-glycoprotein; PI, protease inhibitor; SDS−PAGE, sodium dodecyl sulfate polyacrylamide gels; TBS-T, Tris-buffer saline Tween 20.

Acknowledgment. The authors thank all the surgeons at the Beaujon and Lariboisiere hospitals for their help in obtaining human intestinal tissue samples. We also thank the department of Endoscopy at Beaujon hospital for help during the collection of human intestinal biopsies. Dr. Owen Parkes edited the English text.

MP100015X

(40) Furst, D. Practical clinical pharmacology and drug interactions of low-dose methotrexate therapy in rheumatoid arthritis. *Br. J. Rheum.* **1995**, *34*, 20–25.

(41) Achira, M.; Totsuka, R.; Fujimura, H.; Kume, T. Decreased hepatobiliary transport of methotrexate in adjuvant arthritis rats. *Xenobiotica* **2002**, *32*, 1151–1160.

(42) Grim, J.; Chládek, J.; Martínková, J. Pharmacokinetics and pharmacodynamics of methotrexate in non-neoplastic diseases. *Clin. Pharmacokinet.* **2003**, *42*, 139–151.

(43) Yokooji, T.; Murakami, T.; Yumoto, R.; Nagai, J.; Takano, M. Role of intestinal efflux transporters in the intestinal absorption of methotrexate in rats. *J. Pharm. Pharmacol.* **2007**, *59*, 1263–1270.

(44) Cascorbi, I. Role of pharmacogenetics of ATP-binding cassette transporters in the pharmacokinetics of drugs. *Pharmacol. Ther.* **2006**, *112*, 457–473.

(45) Paine, M.; Fisher, M. Immunochemical identification of UGT isoforms in human small bowel and in Caco-2 cell monolayers. *Biochem. Biophys. Res. Commun.* **2000**, *273*, 1053–1057.

(46) Berggren, S.; Gall, C.; Wollnitz, N.; Ekelund, M.; Karlbom, U.; Hoogstraate, J.; Schrenk, D.; Lennernäs, H. Gene and protein expression of P-glycoprotein, MRP1, MRP2, and CYP3A4 in the small and large human intestine. *Mol. Pharmaceutics* **2007**, *4*, 252–257.

(47) Meier, Y.; Eloranta, J. J.; Darimont, J.; Ismair, M. G.; Hiller, C.; Fried, M.; Kullak-Ublick, G. A.; Vavricka, S. R. Regional distribution of solute carrier mRNA expression along the human intestinal tract. *Drug Metab. Dispos.* **2007**, *35*, 590–594.